Early Stage Assessment

Towards understanding the thermal stability and decomposition mechanism of low-cost protic ionic liquids

Maariyah Y. Suleman,*[a] Agnieszka Brandt-Talbot [b] and Milo Shaffer [c]

Department of Chemistry, Imperial College London, m.suleman@imperial.ac.uk, CID: 0159 2385

Current literature on the thermal stability of ionic liquids is limited, especially for protic ionic liquids. This project investigates the thermal stability of a range of alkylimidazolium and alkylammonium hydrogen sulfate ionic liquids, both protic and aprotic in nature, which found application in biomass processing recently and can be produced at very low cost. This was carried out using TGA, TGA-MS and DIP-MS and NMR spectroscopy to allow identification of decomposition products at both ambient pressure and under vacuum. Thermogravimetric analysis showed that protic and aprotic hydrogen sulfate ionic liquids are more stable than the equivalent chloride and acetate ILs. Under vacuum, the mass spectrum detected a molecular cation for the protic [HC$_4$im][HSO$_4$], while the mass spec of the aprotic [C$_2$C$_1$im][HSO$_4$] only showed molecular fragments, suggesting that the amine evaporates from protic ILs in vacuum. It is unclear whether and how much evaporation contributes to PIL degradation in HSO4 IL under ambient pressure.

Introduction

Ionic Liquids

Ionic liquids (ILs) were first discovered by Walden however, research in this field took off after 1990 whereby ILs became growingly popular.[1,2] ILs are molten salts at temperatures around or below 100 °C.[3,4] In its purest definition, ILs are composed of a discrete anion and a discrete cation, and selecting them separately allows for a large number of combinations.[5] Structurally, ILs have at least one organic component, which is typically the cation.[6] This generally has a bulky and asymmetric structure which results in salts with lower melting points, whilst the anion may be smaller and symmetrical whilst being an organic or inorganic species.[7] Cations most commonly reported have been based on ammonium, phosphonium, imidazolium, and pyridinium.[8] Recent academic research has often focussed on using dialkylimidazolium cations in combination with a variety of anions.[8,9] This has been due to the their low melting points, high thermal stability and in some cases lower toxicity of the starting material.[3,9,10] Common anions used are based on organic salts such as: halides, hexafluorophosphate, tetrafluoroborate, alkyl sulfate, alkyl sulfonates, alkyl phosphates, mesylate, tosylate, triflate, sulphonimides and carboxylates.[8] Some of these cations and anions are shown in fig. 1. Naming of ILs throughout this paper adopts the Welton notation.[11]

Synthesis

ILs are typically formed by transferring a proton or an alkyl group onto an amine or phosphine (fig. 2).[8] Following this, ion exchange occurs namely anion metathesis.[5]
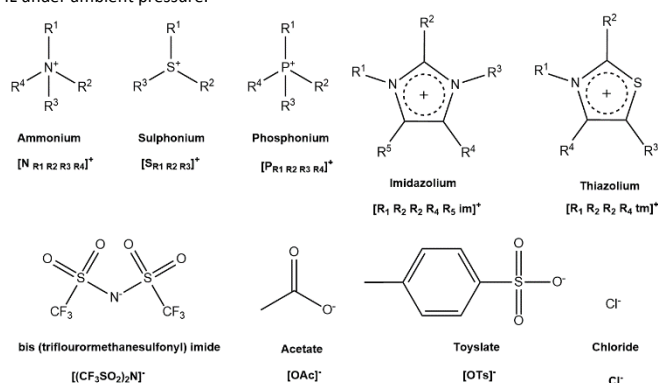

Figure 1 Common cations and anions used for IL synthesis, Notation of these ions are below each structure.

This method of synthesis has a few disadvantages: it requires a solvent, yields are typically below 100% for the alkylation step, ion metathesis produces salt waste which resultantly makes these alkylated ILs (aprotic ILs) more expensive and less green.[5,12] Protic ionic liquids (PILs) are produced by transfer from an acid (organic or inorganic) to an amine. This reaction is simple and efficient without the need for a work-up step allowing for 100 % yields to be obtained, resulting in lower cost.
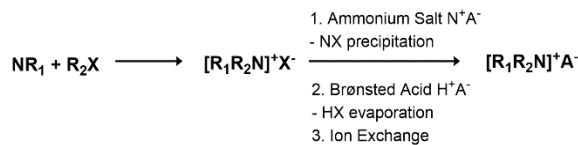

Figure 2 Reaction scheme to show AIL synthesis (top) and PIL synthesis (bottom).

Applications of ILs

ILs have been utilised in several applications including biphasic catalysis, lubricants, electrochemistry and biomass processing usually as an alternative to using molecular solvents.[5,8,21–23,13–

a. Department of Chemistry, Imperial College London, London, SW7 3AZ
b. Email: agi@imperial.ac.uk and mys18@ic.ac.uk
† Footnotes relating to the title and/or authors should appear here.
Electronic Supplementary Information (ESI)
 See DOI: 10.1039/MYS_ESA_19

[20] Several players, such as Shell and BASF have successfully applied ionic liquids in an industrial process, but there remains wider scepticism as ILs are not inherently cheap.[24] Despite demonstrated advantages for using ILs in certain applications, the cost of an IL is a key consideration and can be a barrier to implementation. Ionic liquid such as 1-butyl-3-methylimidazolium bis(trifluoromethanesulfonyl)imide, $[C_4C_1im][N(Tf_2)]$, are prohibitively expensive compared to cheap common organic solvents, which cost between $0.50-1.50/kg.[25] Another key parameter is stability at the processing temperature. For this reason, more low cost ILs must be designed and studied for their properties, in particular thermal stability. A key aspect for reducing the solvent cost is using protic ionic liquids, which will be discussed below.

An example of IL design for both performance and cost is the Ionosolv fractionation of lignocellulosic biomass.[12,26] This processes utilises hydrogen sulfate ILs to extract lignin and hemicellulose from biomass, producing a cellulose-rich solid or pulp and solid lignin.[12,22,26] The ILs used were initially dialkylimidazolium ILs, but it was shown that protic alkylammonium hydrogen sulfate ILs, for example triethylammonium hydrogen sulfate $[N_{2220}][HSO_4]$ and dimethylbutylammonium hydrogen sulfate $[N_{4110}][HSO_4]$, do not reduce performance and are a fraction of the cost.[12] Protic hydrogen sulfate ILs are some of the cheapest ionic liquids that can be conceived, as they are made from sulphuric acid, which costs only $0.07/kg. Despite this, and their highly relevant application in biorefining, $[HSO_4]^-$ based ILs have so far not received much attention besides studies their thermal transition temperatures.[27] Hence, there is limited data regarding their applications and properties.

Protic and aprotic ILs

One method of systematically classifying ILs is determining whether an IL is protic or aprotic. Mentioned previously, for protic ILs, the anion and cation form by proton transfer between a Brønsted-Lowry acid and base (equation 1). This is considered to be a protic ionic liquid (PIL).[8] The difference between PILs and other ILs is the presence of this exchangeable proton and so, the latter non-protic ILs are often called aprotic ionic liquids (AILs).

$$[HB]^+ + A^- \rightleftharpoons HA + B$$
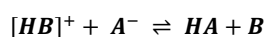
Equation 1   Dynamic equilibria for PILs.

Despite this, it is worth noting some AILs like $[C_4C_1im][HSO_4]$, can still be regarded as a protic solvent providing there is the presence of a proton that can be transferred. For example, ethanol is a protic solvent due to its –OH hydroxyl group, allowing it to form hydrogen bonds with itself and solutes. In this work, protic IL will refer to the acid base complexes, while aprotic ILs are those were the ions are formed with an alkylation step.

For AILs the IL usually completely consists of the cation and anion only, whilst for PILs, the degree of proton transfer is very

important, as partial proton transfer is possible and may lead to the presence of molecular species in the liquid.[28] Indeed, a range of PILs have been reported to have partial proton transfer.[8,29] In an attempt to quantify the degree of proton transfer it has been correlated to ΔpKa between the acid and base precursors.[19,29] This was first investigated by pairing 1-methylimidazolium $[HC_1im]^+$ with a range of weak and strong acids. The study showed that strong acids such as $[N(Tf_2)]^-$ and $[TfO]^-$ resulted in full dissociation, whereas weaker acids (pK$_a$ 0.5 – 4.8) such as formate $[CHOO]^-$ and acetate $[CH_3COO]^-$ had low proton transfer. These were termed 'pseudo-PILs'.[28,30,31] ΔpK$_a$ has also shown to be a good indicator for volatility of an IL, whereby ΔpK$_a$ > 10 can result in vapour pressure similar to that of organic solvents, of the residual acid/base that exists in equilibrium with the ions. It was also suggested by various research groups a ΔpK$_a$ > 10 signifies complete proton transfer.[8,20,29,32,33] However, ΔpK$_a$ is not perfect, as it only valid for dilute aqueous solutions. This is because it was experimentally found protic primary amines have good proton transfer and equilibrium lies towards ionic species; protic tertiary amines have a low proton transfer which was found using a Walden plot illustrating the presence of neutral non-ionic species.[34] This observation was also found computationally using $[N_{3000}]^+$, $[N_{4000}]^+$ and $[N_{4110}]^+$ acetate.[35] Another tool used for measuring the vapour pressure is an integral effusion Knudsen method.[36,37] Vapour pressure measurements have been limited to recording values for AILs as this is experimentally difficult to do. AIL vapour pressures recorded so far have been between 430 − 600 K for $[C_4C_1im][N(CN)_2]$ and $[C_nC_1im][N(Tf_2)]$ where n = 2 − 8.[36,37] No data has been found in literature regarding vapour pressure measurements for PILs.

Table 1   Vapour pressures of common solvents and AILs at 184 °C

Species	Vapour Pressure / Pa	Distil / 1 atm
DMSO[38]	5.6 x 10^4	No
Ethanol [38]	2.0 x 10^6	Yes
$[C_4C_1im][NTf_2]$ [37]	1.3 x 10^{-2}	No
$[C_8C_1im][NTf_2]$ [37]	7.8 x 10^{-3}	No

The vapour phase of ionic liquids

ILs are commonly presumed to have a negligible vapour pressure, due to the strong interionic forces. However, distillation of an ionic liquid was first demonstrated in 2006; A Kugelrohr apparatus was used to experimentally prove be distilled between 200 − 300 °C at reduced pressure (≤ 0.001 mbar) without detection of decomposition products, forcing this statement to be modified.[39] It should be noted, that vapour pressure measurements at ambient conditions have not yet been achieved for PILs and other AILs besides those mentioned above. This is because the distillate produced at ambient pressure are composed of decomposition products as shown in table 2.[39] Subsequently, other methods such as fourier transform ion cyclotron resonance (FT-ICR) coupled with either a line of sight mass-spectrometer (LOSMS) under ultra-high

vacuum or mass-spectrometer (MS) under conditions representative of a reduced pressure distillation setup (10^{-6} – 10^{-4} Pa) have been used to detect species in the vapour phase of ionic liquids.[40,41] Both LOSMS and MS showed that AILs did evaporate as ion pairs and not as single ions or ion pair clusters suggesting the IL used is volatile. PILs have a dynamic equilibrium between the ionic and dissociated form, hence the transferred proton can be returned to the basic anion leading to the formation of a neutral molecular species which may have the potential to evaporate.[39,42]

Table 2 ILs which reportedly decomposed at 300 °C after distillation.[39]

Ionic Liquid	Conditions	Decomposed distillate / %
$[C_4C_1im][N(Tf_2)]$	8 h, 6 mbar	2
$[C_2C_1im][OSO_3C_2H_5]$	5 h, 7 mbar	99
$[PC_{66614}][Decanoate]$	6 h, 7 mbar	95

When surveying the literature, it becomes clear that the vaporisation of PILs has not been studied as extensively as AILs limiting data avilable.[43] Some studies have been conducted to understand the vaporisation products of PILs using fourier transform ion cyclotron resonance mass-spectrometry (FT-ICR-MS) and matrix-isolation FTIR at atmospheric pressures.[43] Results found the presence of ion pairs for $[N_{2220}][OTf]$, $[N_{2220}][N(Tf_2)]$ in the vapour phase, similar to AILs, but also the presence of neutral molecules (acid and base). Raman spectroscopy has also been used to characterise the vapour phase of $[HC_1im][OAc]$, and found neutral molecules which advantageously allows detection of discrete species in situ.[44] Both studies, looked at ΔpK_a and used it to explain the occurrence of either neutral molecules or ion pairs; whereby a lower ΔpK_a favours formation of neutral molecules, and a higher ΔpK_a favours formation of ion-pairs.[43,45]

Thermal stability of ionic liquids

The composition of the vapour phase and ionic liquid stability are intricately linked. For AILs, it has been shown that at an ambient pressure, AIP do not evaporate, but only decomposition products can be found. This is a common behaviour of organic compounds such as glucose which chars in place of decomposition. In addition, many chemical reactions take place at elevated temperatures to speed up reactivity, typically in the range of 60 – 250 °C. Considering this, the thermal stability of ILs is vital for appropriate matching of an IL with its applications. Hence, it is important to understand degradation mechanisms occurring for these ILs.

Studying the thermal stability of ionic liquids

Thermal stability can be studied with thermogravimetric analysis (TGA) using temperature ramping methods with a heating rate of 10 – 20 °C per minute.[9,46,47] This method involves plotting the mass change of a sample as a function of temperature. Using the curves an onset temperature of decomposition (T_{onset}) can be determined, which allows for comparisons of thermal stability between different ILs. . It must be noted that T_{onset} values are obtained after producing two tangents on the curve at the temperature when mass loss is greatest, shown by fig. 3.[48,49] T_{onset} are not suitable to determine the temperature at which decomposition is negligible,[50] which is what is important for industrial applications. In addition, the higher the heating rate the greater the overestimation in T_{onset}.[51] Despite this, TGA is useful for comparing the thermal stability of various ionic liquids, providing the same method and conditions are used.[52,53] This is because the temperature profile is dependent on the atmosphere, heat transfer, heating rate, sample geometry and sample mass.[54]
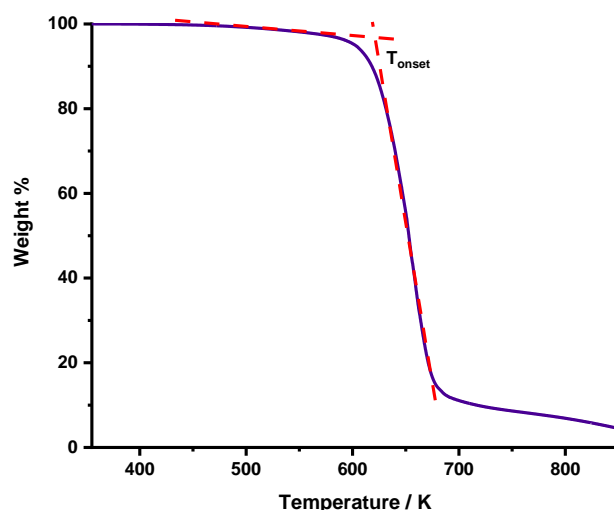

Figure 3 Typical TGA thermograph showing tangents used to obtain T_{onset}

For long-term thermal stability, TGA is also used, but rather than ramping temperatures, an isothermal scan is conducted where a sample is held at a given temperature for a long period of time (2, 15, 20 hours).[9,51,52] The data plotted here is mass loss as a function of time.[51] Information from isothermal measurements have proven to show mass loss over a long period of time can still occur prior T_{onset} and also information on the maximum mass loss observable for a given time.[51] In addition to this, for AILs the temperature where 1 % mass loss over 10 hours ($Td_{0.01/10hr}$) is often calculated using several isothermal slopes to quantitatively study the ILs long-term thermal stability. This is done over a 10-hour period because the 1 % mass loss will otherwise be greatly affected by impurities in the IL and moisture present.

To identify the composition of the vapour phase under atmospheric pressure, the TGA can be coupled with a mass spectrometer (MS). However, few studies have looked at vapour phase components using TGA-MS. Using FT-ICR-MS under non-atmospheric conditions (reduced pressure of 10^{-4} Pa), a study found that the PIL $[HC_1im][OAc]$ vaporised and formed ion-pairs as well decomposition products.[55] No studies looking at the vapour phase of $[HSO_4]^-$ based ILs are available. Generally after heating an IL the decomposition products have been determined using NMR and IR.[9] For dialkylimidazolium ionic liquids, decomposition products were found to form after

deprotonation of the N–C–N carbon atom and dealkylation of the ring itself.[9,56] There have also been inconsistent reports regarding the formation of ion pairs after IL vaporisation because some have shown their formation whilst others have shown their lack of presence. As well as this, there remains limited information on the identification of these decomposition IL products.

Trends in IL stability

For ILs, both the anion and cation have an influence on the thermal stability. It has been postulated, weakly coordinating anions such as bismide provide the highest stability and decomposition temperatures.[23,57] Further to this, during the decomposition process an inversely proportional relationship between IL stability and the stability of an alkyl-anion species has been found.[23] For an imidazolium cation, alkylation of on the C2 carbon has shown to increase the thermal stability of an IL.[48] However, increasing the alkyl chain length does not further increase thermal stability.[48,58] It has also been shown that PILs with a large proton-transfer energy will decompose before they reach their boiling point.[59] PILs with a heterocyclic cation, alkylammonium cation combined with the $[(CF_3SO_2)_2N]^-$ anion often give a $T_{onset} > 300 °C$.[57,60] Whereas a carboxylate anion such as formate has been shown to lower the thermal stability due to the formation of amides via condensation reactions.[61,62] Following the decomposition of ILs, several mechanisms have been proposed.

Decomposition mechanisms

Evaporation is the only physical way of producing measurable mass loss, while several chemical routes are possible. Typical degradation mechanisms are shown in fig. 4. These include: the deprotonation at the C2 position on the imidazole forming an N-heterocyclic carbene; deprotonation of the alkyl chain yielding an alkene and the protonated anion; anion behaving as a nucleophile to deprotonate or dealkylate the imidazole via a S_N2 pathway. These have been corroborated by the coupling of TGA-MS and other techniques such as NMR for the detection of decomposition products.

Decomposition of ammonium and imidazolium based ILs is often endothermic when it is dominated by the loss of an alkyl chain from the cation.[51,63] As stated earlier, alkylation of the imidazolium ring increases the thermal stability suggesting the decomposition mechanism involves deprotonation to produce anion-derived acids and imidazolium-derived carbenes (fig.4, top).[51,64] Techniques such as headspace GC-MS have been used during decomposition of $[C_2C_1im][OAc]$ to confirm the presence of such species; degradation of $[C_2C_1im][N(Tf_2)]$ had alternatively shown multiple anion fragments (CF_3^-, F^-, NH_2^-) which were responsible for consecutive cation decomposition.[65,66]
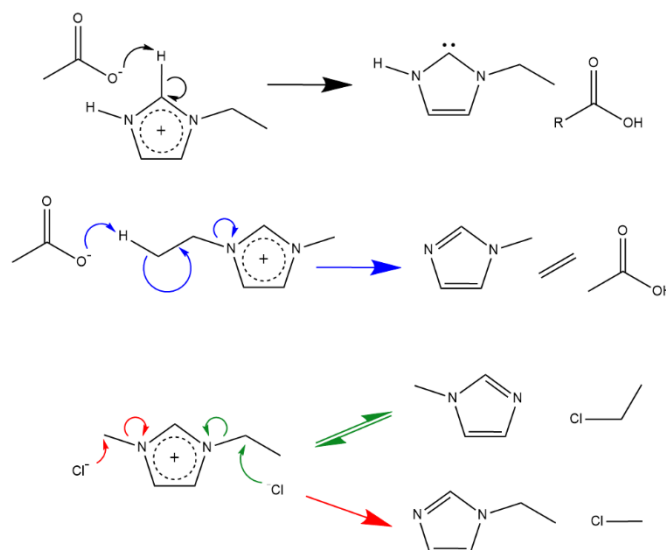

Figure 4 (Black) N-heterocyclic carbene (NHC) formation; (blue) E2 Hofmann elimination; (red, green) S_N2 nucleophilic substitution mechanism.

Decomposition via the reverse Menshutkin reaction

A key degradation reaction is a nucleophilic substitution. It produces two neutral species, sometimes at temperatures as low as 100 °C (fig. 4, bottom).[51] A major degradation product for imidazolium ILs is a neutral alkylimidazole.[67–70] Thermal decomposition of the imidazole ring structure does not occur below 600 °C, hence, no further degradation to form HCN should be observed.[67,71,72] This has been shown for aprotic tetraalkylammonium and dialkylimidazolium halides because alkyl halides have been observed as decomposition products due to the S_N2 mechanism.[71] In a closed system, the reverse Menshutkin reaction forms a dynamic equilibrium with the Menshutkin reaction and so the stability of ILs is linked to the kinetics of both these reactions. The nucleophilicity of the anion and dealkylated imidazole, will affect which of these two reactions will preferentially occur.[51] It was found that nucleophilic anions preferentially attack short alkyl substituents over longer alkyl chains due to steric hindrance; the preference increases the bigger the difference is, which proves this thermal degradation mechanism is kinetically driven.[51,68,71] Additionally, the greater the partial positive charge on a methyl group the more likely it is that a dealkylation occurs at the N-methyl substituent.[55,73]

Clough *et.al* investigated whether the reverse Menshutkin mechanism occurs through S_N1 or S_N2 pathways, (S_N1 refers to the rate determining step being unimolecular and S_N2 having a bimolecular rate determining step).[9,51] For carboxylate ILs, it was found that the S_N2 mechanism primarily occurs at the *N*-methyl substituent for acetate, octanoate and thioacetate anions, while for the fluorinated carboxylate, decarboxylation of the anion was observed.[9] For imidazolium halide ILs it was found to proceed via a S_N2 mechanism.[51] For $[C_2C_1im]X$, the ratio of $[C_1im]$ to $[C_2im]$ increased with decreasing anion size ($I^- > Br^- > Cl^-$) showing smaller anions have a preference $[C_1im]$ compared to $[C_2im]$.[51] A similar study investigated an IL with an allyl substituted imidazolium cation (1-allyl-3-

methylimidazolium) with chloride, bromide and iodide anions. Both 1-methylimidazole and 1-allylimidazole were found to be generated with the amount of 1-allylimidazole increasing as the anion size decreased. The presence of both these products suggests that both S_N1 and S_N2 mechanisms occur, as 1-methylimidazole can only be generated by S_N1.[51] The S_N2 reverse Menshutkin reaction does not occur when there is branching of alkyl chains in halide salts because nucleophilic attack is hindered making the salts more stable.[51]

Decomposition of protic ILs

For PILs it has been shown proton transfer can be poor resultantly giving a ternary mixture of an acid, base and a salt.[33] In addition to this, if the neutral salt is sufficiently volatile at the operating temperatures it will resultantly produce solvent emissions in the composition during a process. Similarly, an excess acid or base will not be involved in proton transfer, regardless if weak or strong acids are used, hence it can be expected a greater composition of volatile products will be produced. To support this, Achinivu *et.al* have shown the mass loss for acetate based PILs is due to the reverse proton transfer forming volatile neutral species.[74] Also, the PILs thermal stability studied, using TGA, varied depending on the cation used where temperatures required for [Pyrr][OAc] > [C_1im][OAc] > [Pyr][OAc].[74] *This* may also affect the decomposition mechanism occurring as the chemistry involved with the neutral species will differ to the ionic counterpart.

Project scope

It is clear that there are a limited number of studies on thermal stability and degradation mechanisms, especially of PILs. It would be greatly beneficial if this data was available for low-cost ILs such as PILs as it would encourage the implementation of ILs in industrial processes. This project aims to study more economically viable ILs, namely [HSO_4]$^-$ based as these ILs have been calculated to give a similar cost to common organic solvents.[12] By gaining a thorough understanding of the decomposition of such ILs and their proposed mechanisms, the process temperatures at which these ILs can industrially operate can be determined.

Experimental

Materials

Table 3   Provenance and purity of the ILs used in the project; All chemicals used as received.

Chemical	Supplier	Purity / %
[C_2C_1im][HSO_4]	Sigma Aldrich	95
[C_2C_1im][OAc]	Iolitec Technologies	95
[C_4C_1im]Cl	Iolitec Technologies	≥ 98
[N_{4110}][HSO_4]	Maariyah Suleman	High
All other ILs	Coby Clark	High

A full list of ILs used have been tabulated in the results section (table 4). ILs not purchased have been synthesised at Imperial College London using commercial starting materials to high purity.

Methods

Moisture and acid : base content

To determine the acid base (anion : cation) ratio of [HSO_4]$^-$ ILs, the moisture content was first determined using a 'V20 Volumetric Karl-Fischer' titrator (Mettler Toledo) and a 'C20 Coulometric Karl-Fischer' titrator (Mettler Toledo). Following this, a 'G20S Compact' titrator was used to determine the acid/base ratio, as it was titrated against a sodium hydroxide standard.

IL synthesis

[N_{4110}][HSO_4] was synthesised via a neutralisation reaction. In a 2L RBF, *N,N*-dimethylbutylamine was measured out and placed in an ice bath. Whilst stirring, 5 M sulfuric acid was added drop wise using a dropping funnel. The acid : base ratio was adjusted by adding more acid or base until a 1:1 ratio was achieved. The IL was then dried using both a rotary evaporator and a Schlenk line.

Thermogravimetric analysis coupled with mass spectrometry (TGA-MS)

Thermogravimetric analysis (TGA) was performed on a 'Mettler Toledo' instrument connected to a 'Hiden analytical HPR 20' mass spectrometer (MS) with a maximum detection of *m/z* 300. Electron ionisation (EI) MS was used with an ionisation energy of 70 eV using a BAR scan of *m/z* 0 – *m/z* 300 in the positive mode. All analysis was carried out under air to give a true representation of any decomposition under atmospheric conditions.

Temperature-ramping TGA-MS experiments were performed using approximately 5 – 10 mg of IL in platinum pans. Method employed: Dry sample at 80 °C for 30 minutes. Ramp temperature to 700 °C at a heating rate of 10 °C.min^{-1} using an air flow of 10 mL.min^{-1}.

Isothermal TGA-MS was performed using 5 – 10 mg of IL in a platinum pan. Method employed: Dry sample at 80 °C for 30 minutes. Ramp temperature up to set temperature$^+$ at a heating rate of 10 °C.min^{-1} using an air flow of 10 mL.min^{-1}. Once set temperature had been reached hold for 390 minutes.

$^+$ *Temperatures used: 240 – 280 °C at +10 °C intervals.*

Data processing was carried out using Origin 2018 software. MS data was obtained as a function of time. To plot this as a function of temperature, a linear-fit was created using TGA temperature data. Following this, MS time values were substituted into this equation to generate temperature values. This was then overlaid with the TGA data.

Direct insertion probe mass spectrometry (DIP-MS)

Direct insertion probe mass spectroscopy (DIP-MS) was carried out on a 'Thermo Finnigan PolarisQ ion trap' mass spectrometer

under vacuum. IL samples were injected into a glass 'Thermo' sample cup until half full then inserted in to the probe tip. Method employed: Dry sample at 80 °C for 2 minutes. Ramp temperature up to a maximum of 450 °C at a heating rate of 10 °C.min^{-1}. Then, hold at 450 °C for 2 minutes. Detection was carried out in both positive and negative modes by alternating the detection once per second. Data processing was carried out using Origin 2018. Raw data from DIP-MS was in the format of time hence it was converted to temperature by using the experimental method. For example, temperature was ramped at a rate of 10 °C.min^{-1} after 2 minutes so temperature values could be extrapolated. Histograms were then produced at the T_{onset} for a given IL.

Decomposition in a closed vessel

Samples of dry IL were heated in 15 ml Ace pressure tubes to 180 °C for 1 hour, 24 hours and 48 hours in a 'Thermo Scientific™ Heratherm™' fan oven. Once cooled to room temperature, samples were prepared for ^{1}H NMR spectral analysis by mixing with DMSO-d_6. ^{1}H NMR spectra were recorded using a Bruker AV400 MHz spectrometer, and spectrums analysed using MestReNova 12.0.

Results and discussion

Acid : Base ratio

The moisture content and acid base ratios were determined as ILs were required to be dry and have a 1:1 ratio. This was because it is known that moisture affects thermal stability, contributing to the irreproducibility of thermographs. This is easily overcome by the drying step prior taking TGA measurements.[51] The acid : base ratio has an effect too as preliminary data have shown that they may affect the volatility of an IL, due to the presence of an excess acid or base in PILs there is a proton transfer between the acid and base.[75]

ILs studied

The ILs used throughout this study have been compared to one another regarding thermal stability. The difference in aprotic and protic [HSO$_4$]$^-$ ILs were of most interest, as PILs are generally cheaper so if the stability of PILs match the stability of the aprotic equivalent it would be advantageous. Hence, both AILs and PILs were included in the investigation. Within each protic/aprotic category the cations used have been imidazolium and ammonium to further show how these affect the stability. In addition to this, both PIL and AILs with varying alkyl chain lengths have been studied to see whether this has an impact. Finally, this project compared several of these [HSO$_4$]$^-$ ILs to the [OAc]$^-$ and Cl$^-$ analogues to determine whether the overall [HSO$_4$]$^-$ ILs are more stable. They also make for good comparisons because the [OAc]$^-$ and Cl$^-$ anion based ILs have been more widely reported in literature for example, in the pretreatment of biomass.

Relative stability of ILs

Relative stability of the ILs chosen for this study was assessed using temperature ramping TGA. The corresponding T_{onset} and $Td_{0.01}$ values listed. From fig. 5, it can be seen that the thermal stability of the investigated ILs strongly depends on the anion used. It can be seen that the order of T_{onset} is with the following [HSO$_4$]$^-$ > Cl$^-$ > [OAc]$^-$. A strong dependence of T_{onset} on the anion agrees with previously reported trends.[10,76–78] As well as this, the order agrees with literature.[9,10] The order is linked to the anions nucleophilicity, hydrogen bond basicity and coordinating ability.[10,48,58,64,79]
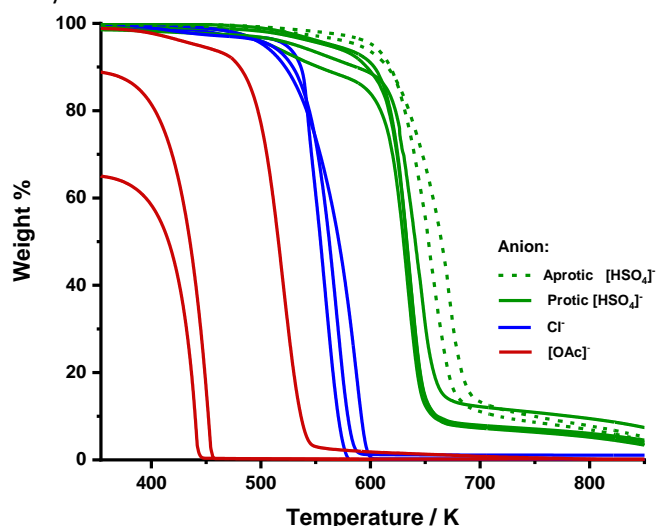

Figure 5 TGA thermographs for several imidazolium [HSO$_4$]$^-$ based PILs (solid green) AIL (dashed green); Aprotic imidazolium and ammonium chlorides (blue); Aprotic and protic imidazolium and protic ammonium acetate ILs (red)

The cation too must be considered. Figure 6. shows the stability for protic and aprotic hydrogen sulfate ILs, and imidazolium based ILs are collectively more stable than ammonium based ILs hence giving large T_{onset} values. This greater thermal stability may be attributed to the delocalised charge for the imidazolium cation and a stable ring. It has been reported the ring will not decompose below 600 °C.[71,72]
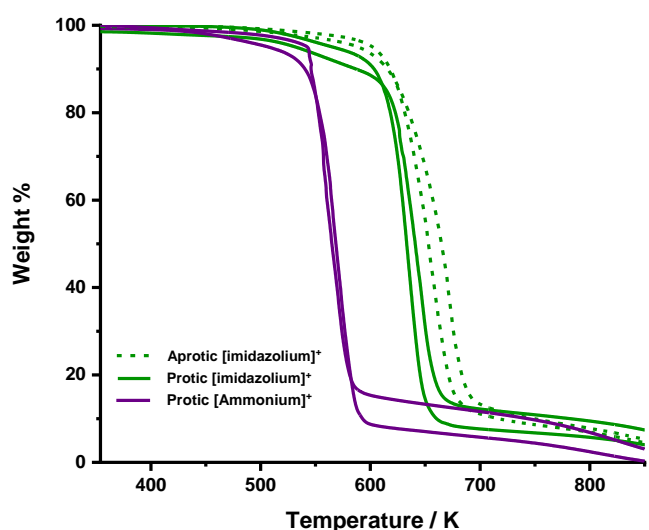

Figure 6 TGA thermographs of hydrogen sulphate ILs using either imidazolium cations: [C$_2$C$_1$im]$^+$ (**6**), [C$_4$C$_1$im]$^+$ (**3**) (dashed green) and [HC$_1$im]$^+$ (**4**), [HC$_4$im]$^+$ (**5a**) (solid green) or ammonium cations; [N$_{2220}$]$^+$ (**2**), [N$_{4110}$]$^+$ (**1**) (purple).

Table 4 Ionic liquids used throughout project and T_{onset}, $Td_{0.01}$ measured under an air atmosphere; acid content of $[HSO_4]^-$ based ILs

Entry	Ionic Liquid	Formula	T_{onset} / °C	$Td_{0.01}$ / °C	Moisture content / %	Acid : Base
1	*N,N*-dimethylbutylammonium hydrogen sulfate	$[N_{4110}][HSO_4]$	277.3	129.6	0.58	0.970
2	*N,N,N*-triethylammonium hydrogen sulfate	$[N_{2220}][HSO_4]$	277.9	155.5	19.39	0.994
3	1-butyl-3-methylimidazolium hydrogen sulfate	$[C_4C_1im][HSO_4]$	342.5	239.2	1.08	1.012
4	1-methylimidazolium hydrogen sulfate	$[HC_1im][HSO_4]$	345.9	80.1	-	-
5a	1-butylimidazolium hydrogen sulfate	$[HC_4im][HSO_4]$	342.5	225.1	0.42	1.003
5b	1-butylimidazolium hydrogen sulfate + 10% acid	$[HC_4im][HSO_4]$	348.3	159.8	0.86	1.120
5c	1-butylimidazolium hydrogen sulfate + 10% base	$[HC_4im][HSO_4]$	339.4	165.4	2.01	0.898
6	1-ethyl-3-methylimidazolium hydrogen sulfate	$[C_2C_1im][HSO_4]$	368.6	205.9	-	1.002
7	1-ethyl-3-methylimidazolium acetate	$[C_2C_1im][OAc]$	222.3	79.8	-	-
8	*N,N*-diethylammonium acetate	$[N_{2200}][OAc]$	151.2	78.2	-	-
9	1-methylimidazolium acetate	$[HC_1im][OAc]$	156.3	79.7	-	-
10	*N,N,N*-triethylammonium acetate	$[N_{2220}][OAc]$	-	-	-	-
11	1-butyl-3-methylimidazolium chloride	$[C_4C_1im]Cl$	271.9	127.1	-	-
12	1-methylimidazolium chloride	$[HC_1im]Cl$	278.6	173.8	-	-
13	*N,N,N,N*-tetraethylammonium chloride	$[N_{2222}]Cl$	265.0	80.0	-	-

These results are as expected for AILs as several investigations have shown that imidazolium AILs are generally more stable than alkylpyridinium, tetraalkylammonium and alkylpiperidinium ILs independent of the anion type.[10] For PILs it was expected the stability would be lower due the proton transfer equilibrium allowing the formation of a ternary mixture, but this was not observed.[33]

Having studied a range of imidazolium ILs, it can be observed whether the alkylation pattern on the imidazolium ring and length of the alky chain has an impact on thermal stability. From the T_{onset} values it is clear the length of the alkyl chain on the protic imidazolium ILs does not dramatically increase thermal stability, certainly to a lesser extent than that shown after changing the type of cation and anion used. Replacing H in $[HC_1im]^+$ (**4**) with an ethyl chain to yield $[C_2C_1im]^+$ (**6**), we observed that T_{onset} increased by 23 °C from 346 °C to 369 °C. However, upon increasing the alkyl chain length (ethyl group to a butyl group, (**6** to **3**)), we observed a decrease in thermal stability, with T_{onset} for $[C_4C_1im]^+$ (343 °C) ≈ $[HC_1im]^+$ (346 °C). Although there is limited data regarding $[HSO_4]^-$ ILs, similar behaviours have been observed for imidazolium cations with $[PF_6]^-$, $[N(Tf_2)]^-$, $[OAc]^-$ and Cl^- anions.[10] Overall, a shorter alkyl chain gives a higher thermal stability whilst a longer alkyl chain decreases thermal stability. This may be because of the greater positive charge on the nitrogen atom adjacent to the alkyl chain which increases dealkylation.[10,80,81]

Long-term thermal stability

TGA isothermal measurements were carried out to study the long-term stability of selected ILs. This is important to understand because industrially ILs may be required to endure high temperatures for long periods of time. For example, [TEA][HSO₄] has been used at elevated temperatures of 150 − 180 °C for pretreatment.[12,26] The recyclability of ILs is also a key consideration. If an IL shows long-term thermal stability with no impact on its performance, it is a great candidate in terms of recyclability. Figure 7. shows the isothermal TGA curves for the PIL $[HC_4im][HSO_4]$ and the AIL $[C_4C_1im][HSO_4]$ at various temperatures. Both these ILs have a T_{onset} around 345 °C (table 4. entry **5a** and **3**), suggesting they have a high thermal stability, yet mass loss is clearly observed below T_{onset}. Degradation occurring below Tonset is well known, and as a rule of thumb, ILs can only be regarded as stable ~100 °C below T_{onset}.[10] This demonstrates the necessity of carrying out long-term TGA measurements alongside determining T_{onset}. For both these ILs the mass loss observed was faster as the temperature increased. The difference in the speed of mass loss between the PIL and AIL was minimal. However, the PIL had a slightly greater speed of mass loss at the same corresponding temperatures shown by the steeper slope. This can be expected for the PIL, as there is an additional mechanism possible, the proton transfer between the acid and base which can form neutral species which are volatile, contributing to the greater mass loss observed. Further kinetic analysis can be carried out using the linear slopes of isothermal scans.[9,10] This is possible providing the decomposition mechanism is pseudo-zeroth order allowing

Arrhenius parameters and the rate of decomposition to be calculated. It can often be assumed decomposition is pseudo-zeroth order, as the decomposition products are typically volatile so their removal allows the concentration of the cation and anion to remain constant.[9] The activation energy for the two ILs will be determined by plotting the time taken for 1 % of decomposition to occur against temperature using the data as future work.[9]
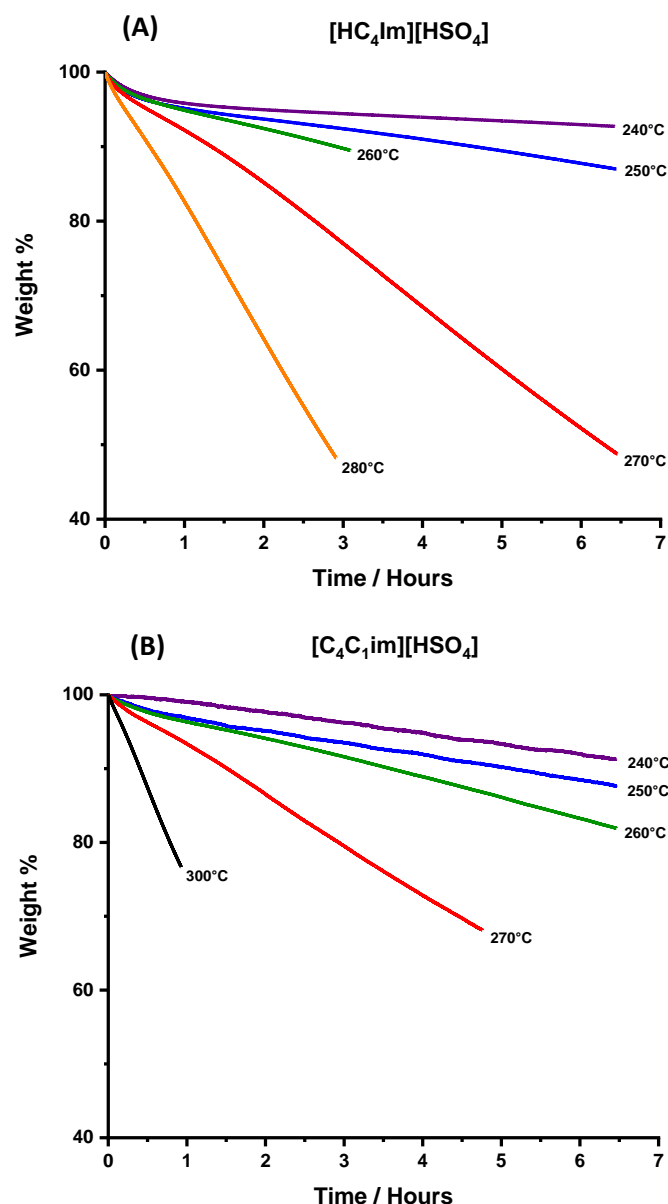
(A)   **[HC$_4$Im][HSO$_4$]**

(B)   **[C$_4$C$_1$im][HSO$_4$]**

Figure 7   TGA Isothermal measurements at varying temperatures for PIL [HC$_4$im][HSO$_4$] (**5a**) and AIL [C$_4$C$_1$im][HSO$_4$] (**3**)

Determining the decomposition products using TGA-MS

To gain insight into the decomposition products the TGA instrument was used with a mass spectrometer coupled to it. By studying the decomposition products, dominant decomposition mechanisms can be proposed. During this study, each IL showed fragmentation occurred after T_{onset}, suggesting there are negligible quantities of volatile species present if any.

Fragments observed have been identified in table 5 based on their m/z. It can be seen that fragments detected from decomposition did not have a *m/z* greater 70. This observation could mean that molecular ions are fragmented into smaller species during the electroionisation process. Alternatively, larger fragments may be present, but they are not transferred from the TGA into the mass spectrometer under the conditions used. This was tested using [C$_2$C$_1$im][OAc] (**7**) because Clough *et.al* has shown the presence of *m/z* 74 and *m/z* 88 hence, it could be concluded whether this observation could also be observed using this studies current TGA-MS instrument. By adding a larger amount of sample, 30 – 50 mg, compared to normal (5 - 10 mg). This mass spectrum showed detection of *m/z* 74, but with a low intensity. Adding such a large amount of sample is not ideal, as adding large quantities of sample for TGA-MS may result in blocking the transfer capillary tube of the MS. The lack of detection of intact ions using TGA-MS does not conclude their absence, but rather the TGA to MS pressure difference can hinder detection of larger molecules in the gaseous phase.[65] Alternative methods have been used to study fragmentation including: computational methods, FTIR and time of flight-MS (TOF-MS) whilst heating ILs to 400 °C.[49,82]

When comparing imidazolium [HSO$_4$]$^-$ based AILs and PILs (fig. 8a), [CO$_2$]$^{+\bullet}$ was produced at two temperatures showing two peaks. This suggests the potential oxidation of the cation in two steps. There also appears to be production of char, which is deposited in the platinum pans at the end of each experiment. Despite drying the ILs prior to measurements, [H$_2$O]$^{+\bullet}$ is continuously detected after T_{onset} suggesting it may have been produced during decomposition although, this is highly unlikely. The majority of the fragments observed are from the decomposition of sulphuric acid namely, [SO]$^{+\bullet}$ and [SO$_2$]$^{+\bullet}$. The NIST chemical database suggests larger masses should also be present (*m/z* 80, 81 and 98), however, these were not observed. Fragments present such as *m/z* 29 may be due to dealkylation of the imidazolium cation via Hofmann elimination, producing an alkene from the cleavage of the N-C bond.

i. $$H_2SO_{4\,(l)} \rightarrow SO_{3\,(g)} + H_2O_{(g)}$$

ii. $$SO_{3\,(g)} \rightarrow SO_{2\,(g)} + \tfrac{1}{2}O_{2\,(g)}$$
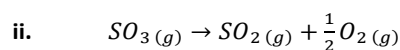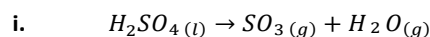
Equation 2   i. Dehydration of sulphuric acid; ii. Reduction of sulphur trioxide

Interestingly *m/z* 40 is observed for both [HC$_4$im]$^+$ and [C$_4$C$_1$im]$^+$, not [C$_2$C$_1$im]$^+$. This fragment has been identified as an azirine fragment which is a product of decomposition of the imidazolium ring itself. In addition to this [C$_4$C$_1$im]$^+$ has an additional fragment peak of *m/z* 41 which is the protonated azirine. This is a fascinating observation because it was previously found the T_{onset} of [HC$_4$im]$^+$ was higher than the T_{onset} for [C$_2$C$_1$im]$^+$ however, when increasing the carbon chain length further, the T_{onset} reduced back to the same value as [HC$_4$im]$^+$. Using this information, it is further emphasised that fragmentation of [C$_2$C$_1$im]$^+$ show a peal for azirine, whereas ILs [HC$_4$im]$^+$ and [C$_4$C$_1$im]$^+$ both show evidence of a lower activation energy for decomposition due to steric and electronic reasons,

as they produce azirines. Interestingly $[C_2C_1im]^+$ does not show the formation of an azirine even with the acetate anion. This further suggests the formation of the azirine may be due to the butyl chain present. However, it must be ensured transfer of gaseous products from the TGA to MS is effective. For $[C_2C_1im][OAc]$ no additional fragments are observed besides at *m/z* 43 which is due to degradation of the acetate anion.
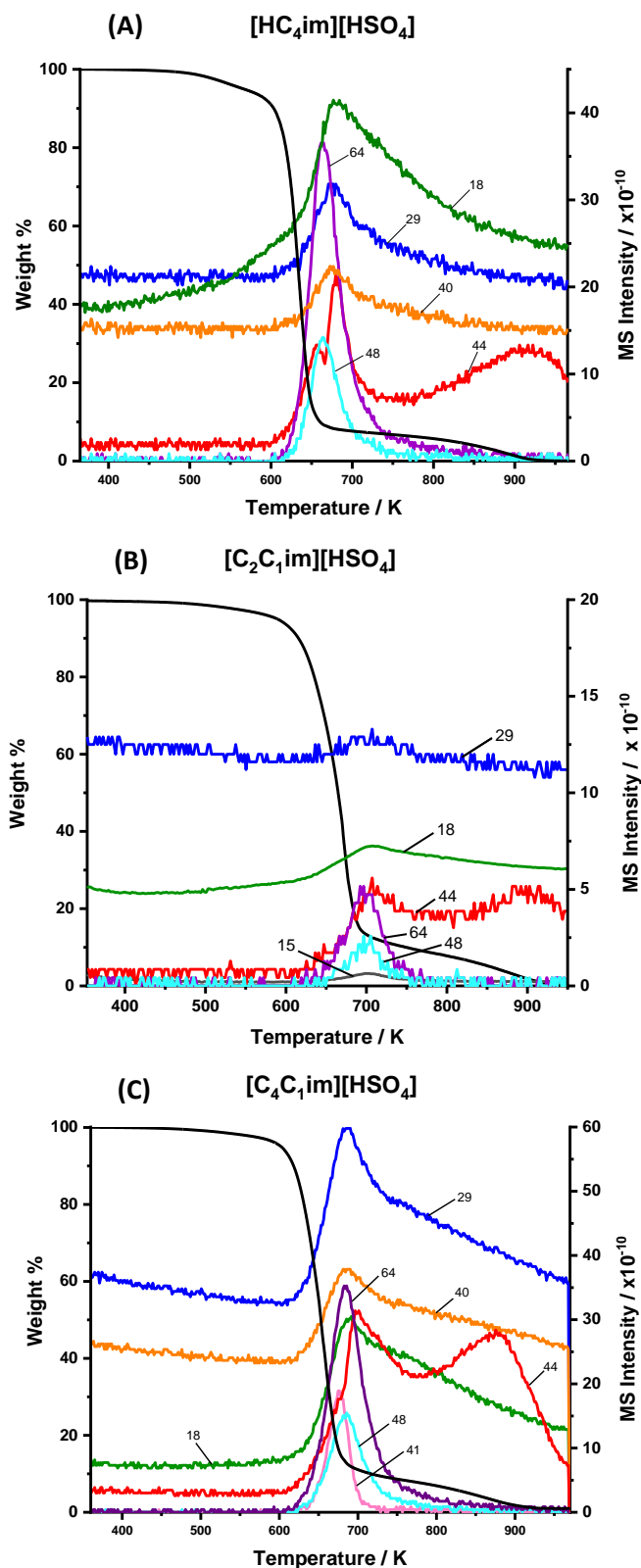
(A) $[HC_4im][HSO_4]$

(B) $[C_2C_1im][HSO_4]$

(C) $[C_4C_1im][HSO_4]$

Figure 8a   TGA-MS for $[HSO_4]^-$ ILs; Protic (A) and aprotic (B,C)

(D) $[C_2C_1im][OAc]$

(E) $[C_4C_1im]Cl$
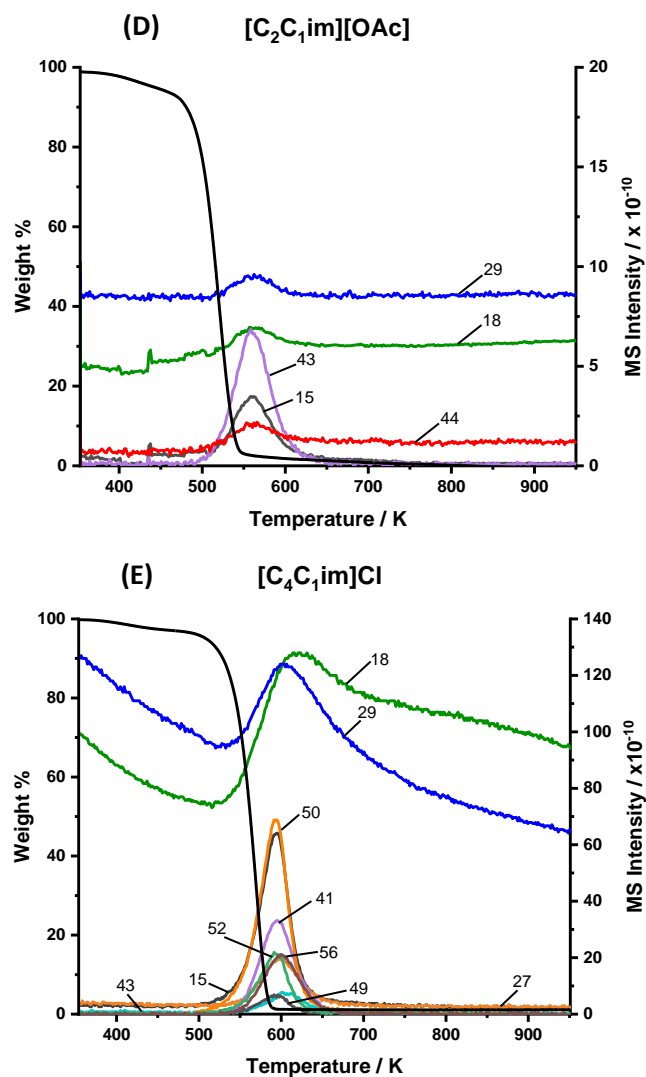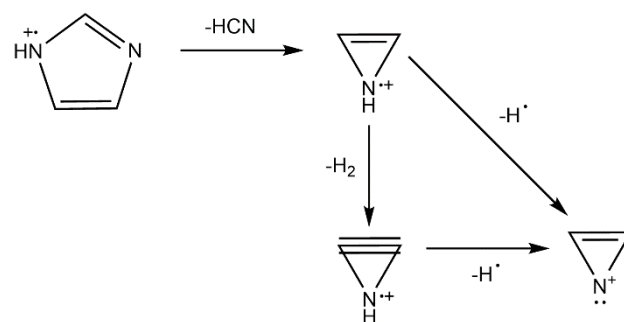
Figure 8b   TGA-MS for acetate IL (D); chloride IL (E)

Figure 9   Fragmentation of imidazole to form an azirine with *m/z* 40

It has been shown that S_N2 nucleophilic substitution occur for $[C_2C_1im][OAc]$ at the methyl substituent on $[C_2C_1im]^+$ where larger fragments with *m/z* 60, 74 and 88 were observed however,[9] however, during this study these fragments were not detected suggesting the vaporised species may have condensed prior detection. $[C_4C_1im]Cl$ was also studied to show how the thermal decomposition products differ here in relation to stability. It is clear that a greater extent of fragmentation is observed with new peaks corresponding to the formation of

$[CH_3Cl^{35}]^{+\bullet}$, $[CH_3Cl^{37}]^{+\bullet}$ via an S_N2 mechanism where Cl^- acts as a nucleophile. There is no evidence for the formation of $[HCl]^{+\bullet}$ which is expected as no protons adjacent to the nitrogen can be abstracted. There is also evidence for an E2 Hofmann elimination reaction occurring, as m/z 56 shows the formation of an alkene from the butyl chain, the $[C_4H_8]^{+\bullet}$ fragment.

Fragments observed for alkylammonium hydrogen sulphate ILs had m/z values same as $[C_2C_1im][HSO_4]$ so plots were excluded (See ESI fig.3). The similar spectra for ILs with different cations suggests cation decomposition is quite advanced in the liquid phase before products go into the vapour phase.

It is interesting that both $[HC_1im][OAc]$ and $[N_{2200}][OAc]$ TGA spectrums show mass loss of 10 – 35 % prior their respective T_{onset} temperature as 156.3 °C and 151.2 °C. However, the MS did not show the presence of any volatile molecular species. (ESI fig.4) This suggests the MS may need to undergo maintenance to ensure detection is accurate and not influencing the results observed. The ionisation technique used employs 70 eV which may be causing fragmentation of the evaporated species. We hence lowered the voltage to 30 eV and were unable to see more fragments, suggesting instrumental errors are present.[75]

Table 5   Assigned decomposition products for TGA-MS for selected m/z values

m/z	Fragment	m/z	Fragment
15	$[CH_3]^{+\bullet}$	43	$[CH_3CO]^{+\bullet}$
18	$[H_2O]^{+\bullet}$	44	$[CO_2]^{+\bullet}$
27	$[C_2H_3]^{+\bullet}$	48	$[SO]^{+\bullet}$
29	$[C_2H_5]^{+\bullet}$	50	$[CH_3Cl^{35}]^{+\bullet}$
36	$[HCl^{35}]^{+\bullet}$	56	$[C_4H_8]^{+\bullet}$
40	$[C_2H_2N]^{+\bullet}$	64	$[SO_2]^{+\bullet}$
41	$[C_2H_2NH]^{+\bullet}$	74	$[CH_3OC(O)CH_3]^{+\bullet}$

Decomposition under vacuum

The vapour phase of hydrogen sulfate based ILs were also studied under vacuum to see if the composition differed from the vapour phase in atmospheric conditions. We used a DIPs MS with a heated stage, allowing decomposition to be monitored at a range of temperatures. The data are plotted as a histograms at the T_{onset} temperature obtained from TGA-MS. In each case, there is evidence to show decomposition of sulfuric acid due to the presence of $[SO_2]^{+\bullet}$. More interestingly, for the PIL $[HC_4im][HSO_4]$ (fig.10) there is an intense peak for the molecular cation suggesting that the base evaporates. The lack of detection for the molecular ion using TGA-MS suggests the vacuum allows the volatile species to escape through evaporation while this does not happen at ambient pressure. For $[HC_4im][HSO_4]$, the presence of a molecular ion and its corresponding fragment from S_N2 nucleophilic substitution was detected giving both $[C_1im]^+$ and $[C_2im]^+$. The fragmentation pattern observed is similar to the already reported MS fragmentation of 1-butylimidazole.[38]

For the AIL $[C_2C_1im][HSO_4]$, similar fragments were observed, however, the intensity of $[C_1im]^+$ was far greater than $[C_2im]^+$. This trend contradicts a previous study that looked at the nucleophilicity using halide anions. The study found the smaller the nucleophilic anion the greater the preference for removing the longer alkyl chain. Although the results do agree with the study, hydrogen sulphate is a large anion and less nucleophilic than halide anions suggesting there is some other reasoning which could be as follows; T_{onset} found the shorter the alkyl chain substituent on the imidazole the greater the stability, similarly the greater intensity of $[C_1im]^+$ may be due to its greater stability than $[C_2im]^+$. Alternatively, there may be both S_N2 nucleophilic substitution and E2 Hofmann elimination of the ethyl chain whereas, the methyl chain can only undergo S_N2 nucleophilic substitution, giving a greater intensity of $[C_1im]^+$ than $[C_2im]^+$ (fig.10).
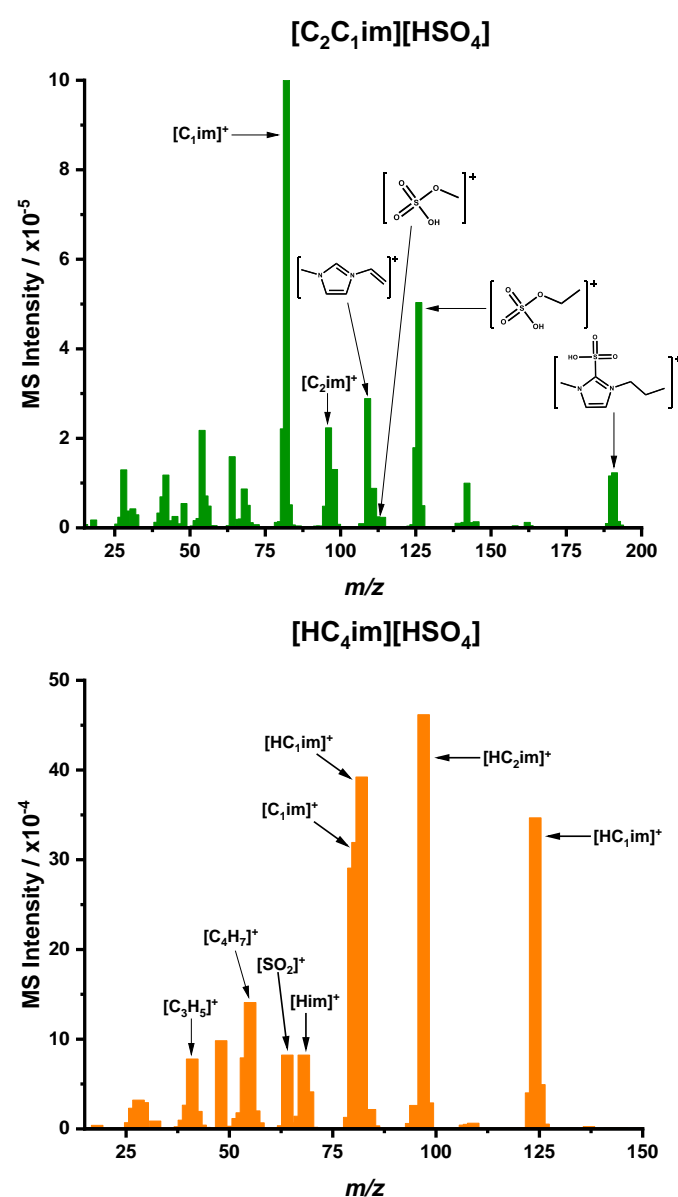
Figure 10a   Histograms for vapour phase components of (**6**) $[C_2C_1im][HSO_4]$ at T_{onset} 368.6 °C (green) and (**5a**) $[HC_4im][HSO_4]$ at T_{onset} 342.5 °C (orange) using DIP-MS in the positive mode.

Detection using the negative mode for $[HC_4im]^+$ has shown the presence of $SO_2]^-$, $[SO_3]^-$ and $[HSO_4]^-$. It is interesting to see presence of the parent anion $[HSO_4]^-$ which suggests the IL under vacuum may exist as an ion-pair. For aprotic $[C_2C_1im]^+$, $[HSO_4]^-$ is not observed suggesting the HSO_4^- anion is more strongly bound to the cation, leading to its decomposition or formation of HSO_3^- based decomposition products proposed in fig. 10a. The proposed products suggest the initial formation of a carbene followed by addition of HSO_3^- on the C2 position. Another proposed structure in the positive mode is ethyl hydrogen sulfate which forms after S_N2 of the ethyl group leaving $[C_1im]^+$. As there is also a peak observed for $[C_2im]^+$, an expected corresponding peak for methyl hydrogen sulfate was observed however, the intensity for this was incredibly low (< 0.5×10^{-6}).
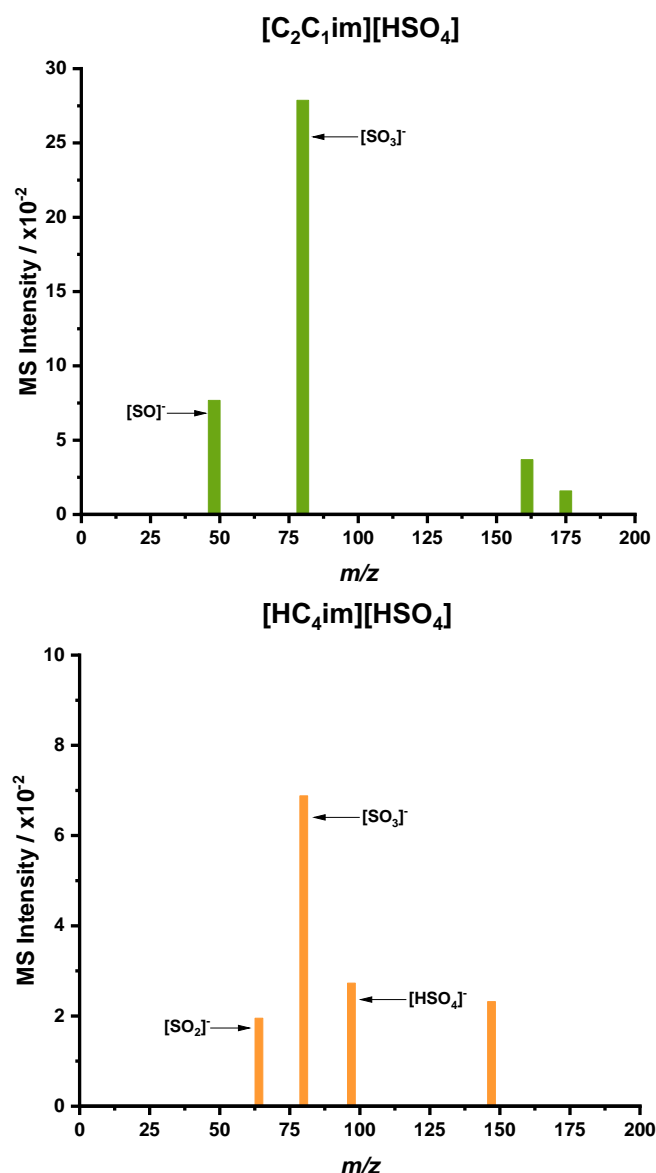
$[C_2C_1im][HSO_4]$

$[HC_4im][HSO_4]$

Figure 10b Histograms for vapour phase components of (**6**) $[C_2C_1im][HSO_4]$ at T_{onset} 368.6 °C (green) and (**5a**) $[HC_4im][HSO_4]$ at T_{onset} 342.5 °C (orange) using DIP-MS in the negative mode.

We also wanted to investigate the decomposition in a closed system in the liquid phase (as opposed in an open system with where decomposition products are removed by vacuum or a gas stream. So far, only $[C_2C_1im][OAc]$ has been investigated, whereby the IL was heated to 180 °C for 0, 1, 24 and 48 h. The product was collected and analysed using ^1H NMR spectroscopy. Figure 11a. shows the signals of the C4 and C5 protons on the imidazolium ring which shows up in the region 7.85 – 7.90 ppm. After heating the IL at 180 °C for 1 h, new peaks were present, including one within the aromatic region at 7.63 – 7.69 ppm. The upfield shift suggests the formation of a dealkylated decomposition product. The formation of this product relative to undecomposed imidazolium can be calculated using the integral of each peak which has been listed in table 4.

Table 4 Ratio of ^1H NMR peak of imidazole $[C_2C_1im]^+$ to decomposition product $[HC_2im]^+$

Heating time / hr	$[C_2C_1im]^+$: $[HC_2im]^+$
0	1 : 0
1	1 : 1
24	1 : 20
48	1 : 2

The relative amount of $[C_2C_1im]^+$ in the liquid decreased whilst the amount of decomposition product $[HC_2im]^+$ increased with a longer heating duration. However, at 48 hrs the ratio of both peaks substantially decreased suggesting further decomposition of the dealkylated imidazole. This can be seen in fig. 11, as the number of peaks between 0.9 – 1.4 ppm dramatically increased. The NMR spectra at 48 h suggests this IL is highly unstable.
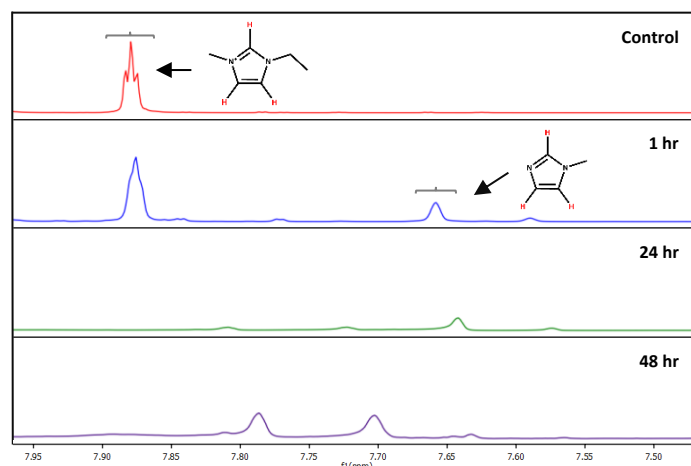

Figure 11a Expanded regions of the ^1H NMR spectrum of $[C_2C_1im][OAc]$ after heating at 180 °C for 0, 1, 24 and 48 hours; Peaks shown in the aromatic region for the imidazole.

Although this study is limited to $[C_2C_1im][OAc]$ it shows NMR can be effectively used to determine the products of decomposition using this experimental setup as results agree with Clough *et.al*. This experiment will be carried out for the hydrogen sulfate ILs used throughout this study.[9]
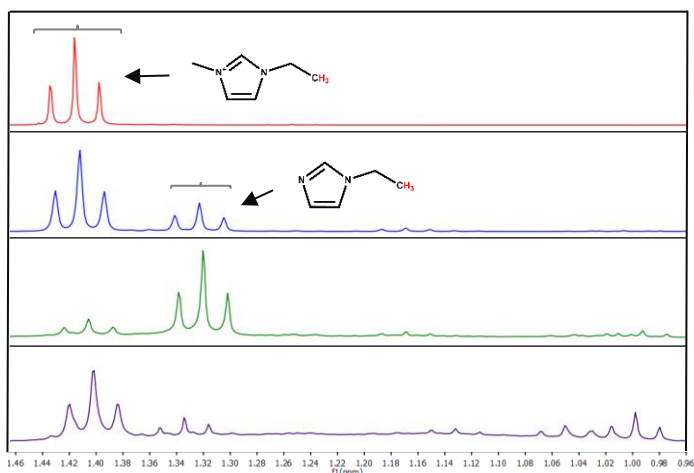
Figure 11b Expanded regions of the ¹H NMR spectrum of [C₂C₁im][OAc] after heating at 180 °C for 0, 1, 24 and 48 hours; Peaks for the formation of decomposition products such as [C₂im]⁺.

Conclusions

In this study, the thermal stability of hydrogen sulfate ionic liquids is studied using multiple techniques both in atmospheric and vacuum conditions and compared to acetate and chloride ILs. It was confirmed the decomposition temperature and mechanism can be affected by both the anion and cation. The thermal stability differences seen by the anion were far greater than the change seen after modifying the type of cation. This is consistent with several reported observations that the thermal stability is highly anion dependant.[10,78] Measuring the T_{onset} temperature of decomposition, it was found that imidazolium rings with an ethyl chain increased thermal stability compared to a butyl chain whilst alkylation with a longer chain decreased thermal stability. The stabilities of hydrogen sulphate ILs affected the degradation products observed under atmospheric conditions, distinctively showing the presence of azirines for imidazolium cation with a butyl chain attached. When chloride was the anion, fragmentation suggests that E2 Hofmann elimination was significant as an alkene fragment was detected. In addition to this, there was evidence for S_N2 nucleophilic substitution due to the alkyl chloride fragment. Different fragments were detected in the vapour phase under vacuum. For the PIL [HC₄im][HSO₄] it was found that the cation could be detected as a molecular ion in the MS, suggesting it is volatilised as base than the AIL analogue for which only fragments of the molecular cation were detected. TGA isothermal measurements for [HC₄im][HSO₄] showed greater mass loss was observed than for aprotic [C₄C₁im][HSO₄] despite both having the same T_{onset} value. This could be due to evaporation from the PIL however, a technique that can discern evaporation and decomposition is necessary for PILs. Following this, ¹H NMR spectra was demonstrated to be a good analytical method in further studying the decomposition of ILs.

Future Work

This study is the beginning of a publishable paper providing more information on the stability and decomposition mechanism of hydrogen sulfate ILs, in particular the [HSO₄]⁻ based PILs. Prior publishing it is clear the gaps in data sets obtained must be complete for example, investigating the T_{onset} and isothermal decomposition of an aprotic ammonium ILs such as [N₂₂₂₂][HSO₄]. As well as this, more DIP-MS data are needed, such that the same cationic species is studied with an acetate and chloride anion allowing for comparisons, as the only variable changing would be the anionic species. This will allow for greater conclusions to be made and allow trends to be observed. It is interesting to see how decomposition mechanisms are occurring, but similar to Clough *et al.*, it would be beneficial to use computational calculations to investigate whether such decompositions mechanisms are in agreement. This may include the modelling of hydrogen-bonding within an IL. More work will involve mathematical analysis of long-term stability by obtaining Arrhenius parameters for decomposition/evaporation and predicting the rate of decomposition of the ILs at any temperature in the system. Alongside this, vapour pressure for select hydrogen sulphate ILs may be calculated. In terms of data processing, the mass spectra obtained from DIP-MS will be plotted in the same format as TGA-MS to allow for a clearer depiction of fragmentation of the IL as a function of temperature. In addition to this, another next step involves utilising NMR spectroscopy to a greater extent to study the stability of ionic liquids in a closed system at relevant processing temperatures.

References

1. Walden, P. Ueber die Molekulargrösse und elektrische Leitfähigkeit einiger geschmolzenen Salze. Bull Acad Imper Sci (St Petersburg) 405–422 (1914).

2. Welton, T. Ionic liquids: a brief history. Biophys. Rev. 10, 691–706 (2018).

3. Wilkes, J. S. & Zaworotko, M. J. Air and water stable 1-ethyl-3-methylimidazolium based ionic liquids. J. Chem. Soc. Chem. Commun. 965 (1992). doi:10.1039/c39920000965

4. Welton, T. Room-Temperature Ionic Liquids. Solvents for Synthesis and Catalysis. (1999). doi:10.1021/CR980032T

5. Abbott, A. P. & McKenzie, K. J. Application of ionic liquids to the electrodeposition of metals. Phys. Chem. Chem. Phys. 8, 4265 (2006).

6. Beyersdorff, T. et al. Electrodeposition from Ionic Liquids - Chapter 2: Synthesis of Ionic Liquids 2 . 1 Nanostructured Metals and Alloys Deposited from. (2017).

7. Welton, T. and P. W. Ionic Liquids in Synthesis. Organic Process Research & Development (Wiley-VCH, 2003). doi:10.1021/op0340210

8. Bronya Clare, Amal Sirwardana, and D. R. M. Synthesis, Purification and Characterization of Ionic Liquids. Current Chemistry 290, (© Springer-Verlag Berlin Heidelberg 2009, 2010).

9. Clough, M. T., Geyer, K., Hunt, P. A., Mertes, J. & Welton, T. Thermal decomposition of carboxylate ionic liquids: trends and mechanisms.

Phys. Chem. Chem. Phys. 15, 20480 (2013).

10. Cao, Y. & Mu, T. Comprehensive Investigation on the Thermal Stability of 66 Ionic Liquids by Thermogravimetric Analysis. (2014). doi:10.1021/ie5009597

11. Niedermeyer, H., Hallett, J. P., Villar-Garcia, I. J., Hunt, P. A. & Welton, T. Mixtures of ionic liquids. Chem. Soc. Rev. 41, 7780 (2012).

12. Brandt-Talbot, A. et al. An economically viable ionic liquid for the fractionation of lignocellulosic biomass. Green Chem. 19, 3078–3102 (2017).

13. Matthias Maase, Klemens Massonne, Klaus Halbritter, Ralf Noe, Michael Bartsch, Wolfgang Siegel, Veit Stegmann, Miguel Flores, Oliver Huttenloch, M. B. Method for the separation of acids from chemical reaction mixtures by means of ionic fluids. 355 (2002). doi:10.1002/3527601791

14. Joglekar, H. G., Rahman, I. & Kulkarni, B. D. The Path Ahead for Ionic Liquids. Chem. Eng. Technol 30, 819–828 (2007).

15. Plechkova, N. V. & Seddon, K. R. Applications of ionic liquids in the chemical industry. Chem. Soc. Rev. 37, 123–150 (2008).

16. Qu, J., Truhan, J. J., Dai, S., Luo, H. & Blau, P. J. Ionic liquids with ammonium cations as lubricants or additives. Tribol. Lett. 22, 207–214 (2006).

17. Zein El Abedin, S. & Endres, F. Electrodeposition of Metals and Semiconductors in Air- and Water-Stable Ionic Liquids. ChemPhysChem 7, 58–61 (2006).

18. Ohno, H. Electrochemical aspects of ionic liquids. (Wiley, 2011).

19. Greaves, T. L. & Drummond, C. J. Protic Ionic Liquids: Properties and Applications. Chem. Rev. 108, 206–237 (2008).

20. MacFarlane, D. R., Pringle, J. M., Johansson, K. M., Forsyth, S. A. & Forsyth, M. Lewis base ionic liquids. Chem. Commun. 1905 (2006). doi:10.1039/b516961p

21. Forsyth, S. A., MacFarlane, D. R., Thomson, R. J. & von Itzstein, M. Rapid, clean, and mild O-acetylation of alcohols and carbohydrates in an ionic liquid. Chem. Commun. 714–715 (2002). doi:10.1039/b200306f

22. Brandt, A., Gräsvik, J., Hallett, J. P. & Welton, T. Deconstruction of lignocellulosic biomass with ionic liquids. Green Chem. 15, 550 (2013).

23. D. J. Adams, P. J. D. and S. J. T. Chemistry in Alternative Reaction Media. Organic Process Research & Development (Wiley & Sons, 2004). doi:10.1021/op034185g

24. A.Ricci. Process for treatment of basil and products thereof. (1970).

25. Passos, H., Freire, M. G. & Coutinho, J. A. P. Ionic liquid solutions as extractive solvents for value-added compounds from biomass. Green Chem. 16, 4786–4815 (2014).

26. Chambon, C. L., Chen, M., Fennell, P. S. & Hallett, J. P. Efficient Fractionation of Lignin- and Ash-Rich Agricultural Residues Following Treatment With a Low-Cost Protic Ionic Liquid. Front. Chem. 7, 246 (2019).

27. and, J.-P. B. & Angell*, C. A. Protic Ionic Liquids: Preparation, Characterization, and Proton Free Energy Level Representation†. (2007). doi:10.1021/JP067589U

28. Greaves, T. L. & Drummond, C. J. Protic Ionic Liquids: Evolving Structure–Property Relationships and Expanding Applications. Chem. Rev. 115, 11379–11448 (2015).

29. Yoshizawa, M., Xu, W. & Angell, C. A. Ionic Liquids by Proton Transfer: Vapor Pressure, Conductivity, and the Relevance of ΔpKa from Aqueous Solutions Masahiro. J. Am. Chem. Soc. 125, 15411–15419 (2003).

30. Kanzaki, R. et al. Acid–Base Property of N -Methylimidazolium-Based Protic Ionic Liquids Depending on Anion. J. Phys. Chem. B 116, 14146–14152 (2012).

31. Doi, H. et al. A New Proton Conductive Liquid with No Ions: Pseudo-Protic Ionic Liquids. Chem. - A Eur. J. 19, 11522–11526 (2013).

32. Yoshizawa M, Belieres JP, Xu W, A. C. Title. in Abst Pap Am Chem Soc 226:U627 (2003).

33. Verdía, P., Brandt, A., Hallett, J. P., Ray, M. J. & Welton, T. Fractionation of lignocellulosic biomass with the ionic liquid 1-butylimidazolium hydrogen sulfate. Green Chem. 16, 1617–1627 (2014).

34. Stoimenovski, J., Izgorodina, E. I. & MacFarlane, D. R. Ionicity and proton transfer in protic ionic liquids. Phys. Chem. Chem. Phys. 12, 10341 (2010).

35. Nasrabadi, A. T. & Gelb, L. D. How Proton Transfer Equilibria Influence Ionic Liquid Properties: Molecular Simulations of Alkylammonium Acetates. J. Phys. Chem. B 122, 5961–5971 (2018).

36. Lovelock, K. R. J., Deyko, A., Licence, P. & Jones, R. G. Vaporisation of an ionic liquid near room temperature. Phys. Chem. Chem. Phys. 12, 8893 (2010).

37. Dzmitry H. Zaitsau et al. Experimental Vapor Pressures of 1-Alkyl-3-methylimidazolium Bis(trifluoromethylsulfonyl)imides and a Correlation Scheme for Estimation of Vaporization Enthalpies of Ionic Liquids. (2006). doi:10.1021/JP060896F

38. Chemistry WebBook. National Institute of Standards and Technology (NIST). Available at: http://webbook.nist.gov/chemistry/.

39. Martyn J. Earle, Jose´ M.S.S. Esperanca, Manuela A. Gilea, Jose´ N. Canongia Lopes, Luı´s P.N. Rebelo, Joseph W. Magee, K. R. S. & J. A. W. The distillation and volatility of ionic liquids. Nature 439, 831–834 (2006).

40. Armstrong, J. P. et al. Vapourisation of ionic liquids. Phys. Chem. Chem. Phys. 9, 982 (2007).

41. João P. Leal, †,‡ et al. The Nature of Ionic Liquids in the Gas Phase. (2007). doi:10.1021/JP073006K

42. M. S. S. Esperança, J. et al. Reviews Volatility of Aprotic Ionic Liquids s A Review. J. Chem. Eng. Data 55, 3–12 (2010).

43. Horikawa, M., Akai, N., Kawai, A. & Shibuya, K. Vaporization of Protic Ionic Liquids Studied by Matrix-Isolation Fourier Transform Infrared Spectroscopy. J. Phys. Chem. A 118, 3280–3287 (2014).

44. Berg, R. W. et al. Raman Spectroscopic Study of the Vapor Phase of 1-Methylimidazolium Ethanoate, a Protic Ionic Liquid. J. Phys. Chem. A 114, 10834–10841 (2010).

45. Zhu, X., Wang, Y. & Li, H. Do all the protic ionic liquids exist as molecular aggregates in the gas phase? Phys. Chem. Chem. Phys. 13, 17445 (2011).

46. Huddleston, J. G. et al. Characterization and comparison of hydrophilic and hydrophobic room temperature ionic liquids incorporating the imidazolium cation. Green Chem. 3, 156–164 (2001).

47. Valkenburg, M. E. V., Vaughn, R. L., Williams, M. & Wilkes, J. S. Thermochemistry of ionic liquid heat-transfer fluids. Thermochim. Acta 425, 181–188 (2005).

48. Ngo, H. L., LeCompte, K., Hargens, L. & McEwen, A. B. Thermal properties of imidazolium ionic liquids. Thermochim. Acta 357–358, 97–102 (2000).

49. Chan, B., Chang, N. & Grimmett, M. The synthesis and thermolysis of imidazole quaternary salts. Aust. J. Chem. 30, 2005 (1977).

50. Crosthwaite, J. M., Muldoon, M. J., Dixon, J. K., Anderson, J. L. &

Brennecke, J. F. Phase transition and decomposition temperatures, heat capacities and viscosities of pyridinium ionic liquids. J. Chem. Thermodyn. 37, 559–568 (2005).

51. Maton, C., De Vos, N. & Stevens, C. V. Ionic liquid thermal stabilities: decomposition mechanisms and analysis tools. Chem. Soc. Rev. 42, 5963 (2013).

52. Wooster, T. J., Johanson, K. M., Fraser, K. J., MacFarlane, D. R. & Scott, J. L. Thermal degradation of cyano containing ionic liquids. Green Chem. 8, 691 (2006).

53. Wilkes, J. S. Properties of ionic liquid solvents for catalysis. J. Mol. Catal. A Chem. 214, 11–17 (2004).

54. M. Kosmulski, J. G. and J. B. R. No Title. Thermochim. Acta 412, 47–53. (2004).

55. Reddy, R. G. Novel applications of ionic liquids in materials processing. J. Phys. Conf. Ser. 165, 012076 (2009).

56. Zhou, Z.-B., Matsumoto, H. & Tatsumi, K. Cyclic Quaternary Ammonium Ionic Liquids with Perfluoroalkyltrifluoroborates: Synthesis, Characterization, and Properties. Chem. - A Eur. J. 12, 2196–2212 (2006).

57. Bicak, N. A new ionic liquid: 2-hydroxy ethylammonium formate. doi:10.1016/j.molliq.2004.03.006

58. Fredlake, C. P., Crosthwaite, J. M., Hert, D. G., Aki, S. N. V. K. & Brennecke, J. F. Thermophysical Properties of Imidazolium-Based Ionic Liquids. (2004). doi:10.1021/je034261a

59. Belieres, J.-P., Angell*, C. A., Belieres, J.-P. & Angell, C. A. Protic Ionic Liquids: Preparation, Characterization, and Proton Free Energy Level Representation. (2007).

60. Hirao, M., Sugimoto, H. & Ohno, H. Preparation of Novel Room-Temperature Molten Salts by Neutralization of Amines. Journal of The Electrochemical Society 147, (2000).

61. Tamar L. Greaves, † et al. Protic Ionic Liquids: Solvents with Tunable Phase Behavior and Physicochemical Properties. (2006). doi:10.1021/JP068102K

62. Susan, M. A. B. H., Noda, A., Mitsushima, S. & Watanabe, M. Brønsted acid–base ionic liquids and their use as new materials for anhydrous proton conductors. Chem. Commun. 938 (2003). doi:10.1039/b300959a

63. Kroon, M. C., Buijs, W., Peters, C. J. & Witkamp, G.-J. Quantum chemical aided prediction of the thermal decomposition mechanisms and temperatures of ionic liquids. Thermochim. Acta 465, 40–47 (2007).

64. Huddleston, J. G. et al. Characterization and comparison of hydrophilic and hydrophobic room temperature ionic liquids incorporating the imidazolium cation. Green Chem. 3, 156–164 (2001).

65. Chen, Y., Cao, Y., Shi, Y., Xue, Z. & Mu, T. Quantitative Research on the Vaporization and Decomposition of [EMIM][Tf 2 N] by Thermogravimetric Analysis–Mass Spectrometry. (2012). doi:10.1021/ie300247v

66. Wendler, F., Todi, L. N. & Meister, F. Thermostability of imidazolium ionic liquids as direct solvents for cellulose. Thermochim. Acta (2012). doi:10.1016/j.tca.2011.11.015

67. K. J. Baranyai, G. B. Deacon, D. R. MacFarlane, J. M. Pringle and J. L. Scott, Aust. J. Chem., 2004, 57, 145–147.

68. A. Chowdhury and S. T. Thynell, Thermochim. Acta, 2006, 443, 159–172.

69. Y. Hao, J. Peng, S. Hu, J. Li and M. Zhai, Thermochim. Acta, 2010, 501, 78–83.

70. B. K. M. Chan, N. H. Chang and M. R. Grimmett, Aust. J. Chem., 1977, 30, 2005–2013.

71. H. Ohtani, S. Ishimura and M. Kumai, Anal. Sci., 2008, 24, 1335–1340.

72. C. G. Begg, M. R. Grimmett and P. D. Wethey, Aust. J. Chem., 1973, 26, 2435–2446.

73. P. A. Hunt, J. Phys. Chem. B, 2007, 111, 4844–4853.

74. Achinivu, E. C., Howard, R. M., Li, G., Gracz, H. & Henderson, W. A. Lignin extraction from biomass with protic ionic liquids. Green Chem. 16, 1114–1119 (2014).

75. Krishan S. Gosai. Examining the volatility and decomposition of sulfate ionic liquids with temperature. (2018).

76. Hugar, K. M., Kostalik, H. A. & Coates, G. W. Imidazolium Cations with Exceptional Alkaline Stability: A Systematic Study of Structure–Stability Relationships. (2015). doi:10.1021/jacs.5b02879

77. Makhoukhi, B., Villemin, D., Amine Didi, M. & Didi, M. A. Synthesis of bisimidazolium–ionic liquids: Characterization, thermal stability and application to bentonite intercalation. J. Taibah Univ. Sci. 10, 168–180 (2016).

78. Maria Siedlecka, E., Czerwicka, M., Stolte, S. & Stepnowski, P. Stability of Ionic Liquids in Application Conditions. Curr. Org. Chem. 15, 1974–1991 (2012).

79. King, A. W. T. et al. Relative and inherent reactivities of imidazolium-based ionic liquids: the implications for lignocellulose processing applications. RSC Adv. 2, 8020 (2012).

80. Arellano, I. H. J., Guarino, J. G., Paredes, F. U. & Arco, S. D. Thermal stability and moisture uptake of 1-alkyl-3-methylimidazolium bromide. J. Therm. Anal. Calorim. 103, 725–730 (2011).

81. Song, Y., Xia, Y. & Liu, Z. Influence of Cation Structure on Physicochemical and Antiwear Properties of Hydroxyl-Functionalized Imidazolium Bis(trifluoromethylsulfonyl)imide Ionic Liquids. Tribol. Trans. 55, 738–746 (2012).

82. Seeberger, A., Andresen, A.-K. & Jess, A. Prediction of long-term stability of ionic liquids at elevated temperatures by means of non-isothermal thermogravimetrical analysis. Phys. Chem. Chem. Phys. 11, 9375 (2009).